An Archaeochemical Microstructural Study on Koryŏ Inlaid Celadon

Seung Wook Ham, Il-wun Shim, Young Eun Lee, Ji Yoon Kang, and Kyongshin Koh*

Department of Chemistry, Chung-Ang University, Seoul 156-756, Korea
Received May 21, 2002

With the invention of the inlaying technique for celadon in the latter half of the 12th century, the Koryŏ potters reached a new height of artistic and scientific achievement in ceramics chemical technology. Inlaid celadon shards, collected in 1991 during the surface investigation of Kangjin kilns found on the southwestern shore of South Korea, were imbedded in epoxy resin and polished for cross-section examination. Backscattered electron images were taken with an electron microprobe equipped with an energy dispersive spectrometer. The spectrometer was also used to determine the composition of micro-areas. Porcelain stone, weathered rock of quartz, mica, and feldspar composition were found to be the raw material for the body and important components in the glaze and white inlay. The close similarity between glaze and black inlay in the microstructure suggests that the glaze material was modified by adding clay with high iron content, such as biotite, for use as black inlay. The deep soft translucent quality of celadon glaze is brought about by its microstructure of bubbles, remnant and devitrified minerals, and the schlieren effect.

Key Words : Microstructure, White inlay, Black inlay, Koryŏ inlaid celadon, Korean traditional ceramics

Introduction

Some of the world's most coveted and admired masterpieces of ceramics art were produced in Korea during the Koryŏ and Chosŏn dynasties. They were the result of highly sophisticated technology that was basically chemical in nature. The ability and skill to select and treat materials for body, glaze, and decorative properties, to attain the high temperature necessary for proper vitrification of stoneware and porcelain, and to control the atmosphere in the kiln for developing desired glaze colors made ceramics technology the premier high technology of that time. Korea and China were the only countries that possessed such an advanced chemical technology as early as the ninth century.

Ceramic products are highly complicated multicomponent heterogeneous systems that have been the subject of intense chemical research for centuries. The research began in earnest several decades before the Chemical Revolution when Italians, Germans, French and the English raced to produce hard-paste white porcelain, "white gold", imported from China. Rene de Reaumur, Jean Hellot, and Pierre Joseph Macquer were among numerous chemists who were instrumental in applying successfully chemical principles to ceramics production.[1]

The science of Korean stoneware and porcelain is just beginning to be unfolded. Unlike their Chinese counterparts, Korean stoneware first became the subject of analysis in the 1970's, actively only in the last decade.[2-6] Though late in arrival by several centuries, the current interest in Korean ceramics both as art and science runs deep and wide. Also, modern sophisticated instruments and techniques are enabling these objects to reveal themselves in detail as never before. Compositional studies on Koryŏ celadon,[7,8] *punch'ŏng*,[9] and Chosŏn whiteware[9,10] have been reported by the authors. Recently a microstructural study on *punch'ŏng* was presented,[11] and in this paper a microstructural image and compositional analysis with EPMA (electron probe microanalyzer) on the inlaid celadon from Kangjin is presented. In Kangjin, in the southwestern tip of South Korea, the inlay technique was invented and blossomed into Koryŏ masterpieces.

Inlaying technique is the second of two original achievements and an extension of the first Koryŏ potters in Kangjin made in the eleventh and twelfth centuries. Their first achievement of jade-like *pisaek* glaze produced celadon masterpieces that were already recognized as the first under heaven.[12] On many of the pieces were incised such figures as lotus buds and peony flowers, which showed through the clear blue-green glaze. In inlay decorative techniques the incised lines and planes were filled with white or black clay material to contrast with the gray body color. With this second invention the craftsmen creativity reached a new height producing such famous pieces as the *meipyong*, uniquely decorated with flying cranes and clouds. In Figure 1(a) is shown another popular type of celadon, a vase with chrysanthemum flowers in white and black inlay. Later in the fourteenth century several modifications in the incision and filling techniques led to another unique Korean ceramic art *punch'ŏng.* The use of only simple earthy material rather than colorful overglaze pigments is appreciated today as quintessentially oriental.

Experimental Section

Inlay celadons were produced mostly in Sadangni kilns in Kangjin during the 13th and 14th centuries. The kilns were investigated in depth in 1991 by a team from Haegang Ceramics Museum, who provided the ceramic shards for this analysis. Typical shards used in the study are shown in Figure 1(b).

The shards were embedded in epoxy resin and polished for

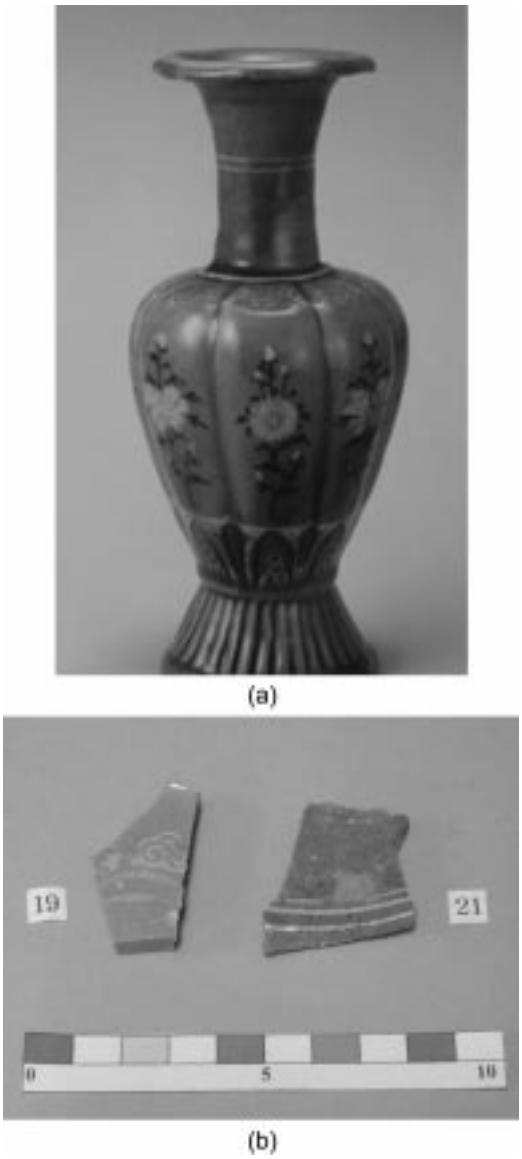

Figure 1. Inlaid celadon produced in the latter half of Koryŏ dynasty. (a) A vase decorated with white and black inlay; (b) Typical shards from Kangjin kiln that were analyzed in this study for the microstructural characteristics.

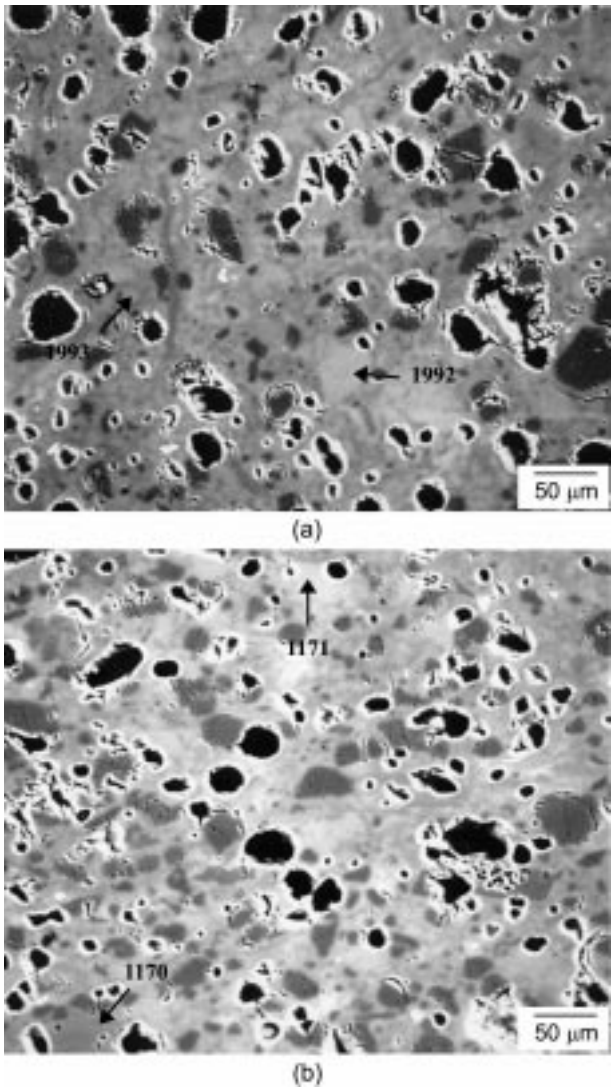

Figure 2. Backscattered electron images (BEI) of body. (a) Shard sample 22 (CE11-3); (b) 169 (S-27-9).

cross-section examination. The BEI (backscattered electron images) and determination of the composition of micro-areas were made at Hoffman Geological Laboratory of Harvard University on a Cameca MBX electron microprobe equipped with a Tracor Northern TN-5502 Energy Dispersive Spectrometer and a stage automation system. The geological standard, detection limit, and counting error used for each element were as follows: for Si quartz, 0.04 wt.%, and 0.30 %; for Al anorthite, 0.03 wt.%, and 0.15-0.30%; for Fe hematite, 0.06 wt.%, and 0.04-0.07%; for Mg enstatite, 0.02 wt.%, and 0.02%; for Ca anorthite, 0.04 wt.%, and 0.05-0.16%; for Na albite, 0.03 wt.%, and 0.05%; for K microcline, 0.03 wt.%, and 0.04-0.10%; for Ti rutile, 0.08 wt.%, and 0.20-0.40%; for Mn tephroite, 0.05 wt.%, and 0.02%; for P apatite, 0.04 wt.%, and 0.03%. Bence-Albee85 and Armstrong alpha values were used for matrix correction. Beam energy was 15 keV and beam current, 14 nA. Various beam sizes of 3, 6, and 15 μm and in some cases a point beam were used for measuring microstructural composition.

Results and Discussion

Body. Hard-paste porcelain material is basically composed of three materials, each providing different properties: clay with plasticity, feldspar that facilitates melting and mixing of different mineral components, and refractory quartz, which prevents collapsing of shaped wares from over-melting. The plasticity necessary for forming is provided, as expected, by kaolinite and other similarly structured clay minerals in raw ceramic materials from the loess plains of northern China and in various western formulations for the body ingredients. However, the plastic component in *tosuk* (pottery stone or porcelain stone), the naturally occurring weathered rocks from which the overwhelming majority of Korean stoneware and porcelain and those from southern China are produced is mineral with mica structure in various forms, such as musco-

Table 1. Composition of micro-areas in body measured by EPMA

Phase	Sample no.	Analyzed point	Normalized oxide concentration (wt.%)										
			SiO_2	Al_2O_3	Fe_2O_3	MgO	CaO	Na_2O	K_2O	TiO_2	MnO	P_2O_5	SO_3
body													
matrix 1	22(CE11-3)	1193	56.85	35.33	2.76	0.79	0.44	0.78	2.44	0.53	0.03	0.03	0.02
(Al-rich silicate:	166(S-27-6)	1161	58.92	32.26	2.73	0.86	0.27	1.01	3.46	0.42	0.04	0.03	–
muscovite)	169(S-27-9)	1170	54.20	40.68	1.38	0.42	0.22	0.52	2.41	0.12	0.02	0.02	–
matrix 2	22(CE11-3)	1192	68.00	18.76	5.10	1.28	1.22	1.51	3.86	0.19	0.04	0.03	–
(K-rich silicate:	166(S-27-6)	1159	67.93	19.31	2.81	0.76	0.82	2.23	6.06	0.04	0.03	0.01	–
K-feldspar)		1160	68.58	18.91	4.53	1.33	0.50	1.32	4.67	0.12	0.03	-	–
	169(S-27-9)	1171	66.05	23.15	3.46	1.12	0.56	1.07	4.10	0.36	0.09	0.03	–
glaze													
K-feldspar relict	166(S-27-6)	1145	65.85	16.19	0.65	0.48	9.31	1.11	6.22	0.00	0.18	0.01	–
(within the aggregation of quartz grains)		1148	66.86	14.87	0.40	0.61	10.50	0.94	5.40	0.00	0.20	0.21	–
wollastonite	166(S-27-6)	1144	51.41	0.10	0.08	0.04	47.99	0.01	0.10	0.00	0.09	0.18	–
muscovite relict	169(S-27-9)	1168(core)	50.59	39.66	0.18	0.14	3.00	0.80	5.52	0.04	0.04	0.03	–
		1169(rim)	50.10	30.71	0.24	0.28	16.05	0.98	1.26	0.02	0.06	0.30	–
schlieren effect	22(CE11-3)	1187	57.76	12.76	1.77	2.00	21.67	0.26	2.64	0.00	0.42	0.71	–
light		1188	54.83	13.49	2.00	2.24	23.77	0.31	1.82	0.00	0.54	1.01	–
		1191	56.27	13.01	1.73	2.22	22.57	0.31	2.25	0.15	0.48	0.98	0.02
dark		1189	59.54	13.25	1.41	1.73	19.33	0.34	3.34	0.00	0.36	0.68	–
		1190	56.88	13.53	1.94	2.01	21.40	0.33	2.32	0.18	0.49	0.90	0.02
white inlay													
muscovite relict	166(S-27-6)	1157	52.25	39.44	2.80	0.73	0.17	0.62	3.86	0.06	0.02	0.05	
		1158	50.00	33.30	6.77	3.49	0.19	0.77	5.39	–	0.09	0.01	–
	133b(DF12-2)	1197	51.27	39.59	0.97	0.31	0.88	0.12	6.28	0.02	0.06	0.31	0.18
comparison of	19(CI11-2)	white inlay	59.50	34.40	1.22	0.33	0.55	0.27	3.34	0.08	0.03	0.07	0.20
intergrade with	white 4	glaze	59.08	13.51	1.34	2.27	19.51	0.39	2.53	0.12	0.41	0.82	
inlay and glaze		intergrade	61.44	17.85	1.75	1.73	12.48	0.38	3.48	0.12	0.31	0.47	0.01
apatite	22(CE11-3)	1185	14.88	2.70	0.85	0.71	49.79	0.09	0.16	–	0.30	30.51	–
black inlay													
matrix	166(S-27-6)	1166	51.98	22.20	12.63	2.50	6.21	0.78	2.07	1.05	0.25	0.31	–
		1167	55.28	19.70	12.06	2.40	5.47	0.83	2.60	0.74	0.22	0.71	–
anorthite	169(S-27-9)	1165	47.73	32.72	0.63	0.15	17.13	0.85	0.41	0.10	0.04	0.23	–
spinel	22(CE11-3)	1172	4.26	56.66	30.44	7.40	0.27	0.03	0.28	0.36	0.23	0.04	0.03
		1173	2.18	58.87	30.45	7.77	0.13	0.02	0.11	0.23	0.20	0.02	0.01
spinel	166(S-27-6)	1151	1.61	58.13	33.34	6.61	0.08	–	0.11	–	0.11	–	–

vite, biotite, sericite and illite.

These various muscovite-type minerals are formed as intermediary minerals in granite rocks whose Na- and K-rich feldspars are transformed to clays of aluminous silicates without any alkaline elements. Various amounts of Na and K remaining in these intermediary minerals act as flux, while the extreme fineness of the grains and their platy characteristics make them plastic. Feldspars that remain unchanged facilitate the fluxing, while a small amount of the clay end product provides further plasticity. Quartz is abundantly present in these granite rocks in all stages of transformation. Thus *tosuk* contains all the necessary ingredients in its natural state for stoneware and porcelain, allowing Korean and southern Chinese potters to make their wares *tanmi*, single-taste, with this earthen material alone, only after refining it through the mechanical steps of pounding, floating, and kneading.

Two images of body in Figure 2 show the microstructural characteristics of inlaid celadon that was made with *tosuk*. Most of the original minerals and pores have disappeared in the process of vitrification and densification. Unlike for glass, the firing is stopped before the ceramics bodies are fully and homogeneously vitrified, and the microstructural features were “frozen-in” when the heating is stopped.

The matrix consists of two irregularly mixed glassy phases, which reflect the composition of the original minerals. As shown in Table 1 the lighter phase, represented by the points 1171 and 1192, is rich in potassium and low in aluminum oxide, as its main component was feldspars, especially of K type (microcline or orthoclase). The darker phase, represented by the points 1170 and 1193, is derived from high aluminum muscovite minerals.

The darkest (black) irregularly shaped hollow sites are the pores, much fewer in number and more round than the pores

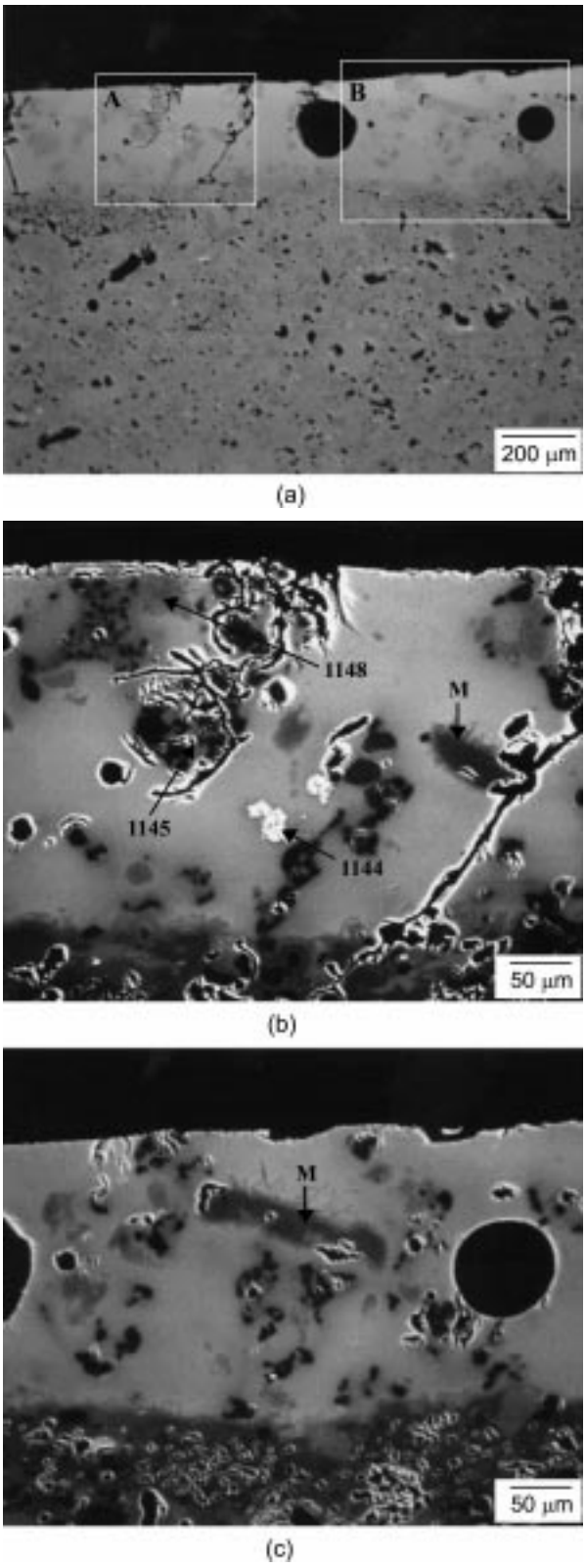

Figure 3. Backscattered electron images of the sample 166 (S-27-6). (a) Body and glaze; (b) A higher magnification of area A; (c) A higher magnification of area B.

present in raw material before the firing. The dark gray grains are quartz, most of which retained their shape. Some have crackled, especially around the edges during the cooling process. Mullite, both primary and secondary formed from high-aluminum mineral and feldspar, respectively, when the wares are fired above 1050 °C, is not shown in these images. Usually too fine and small to be seen in electron images, their peaks occur prominently along with those of quartz in X-ray diffraction patterns of the fully fired bodies.

Glaze. The glaze is much further vitrified than the bodies due to the higher content of flux, provided chiefly by CaO. Some highly fluxed glazes are completely vitrified, appearing clear and transparent as glass. Some contain mineral grains that have been dissolved only partially or even not at all during the firing process and some that have devitrified newly during the cooling process. Most contain bubbles of varying size and quantity. They are pockets of gases, which formed and flowed toward the surface during the vitrification process and were trapped when the firing was stopped.

The glaze on inlaid celadon usually contains bubbles and both remnant and devitrified minerals. In fact, the characteristic translucent quality of celadon glaze comes from this microstructure of bubbles and mineral grains, which scatter and diffract light. The glaze of the shard 166 (S-27-6) shown in Figure 3 is an example of celadon glaze that has several varieties of much relict and devitrified minerals. Figure 3(a) of the image magnified only by about 70 times shows the overall difference between the body and glaze microstructure. Relatively large and also tiny bubbles occur in the glaze, while many pores of various size and shape are in the body. Dark thin lines that go through the entire glaze shown on the left edge and also on the right borderline of the area boxed as A are the image of crackles that are found often in glazes of celadon and other traditional stoneware and porcelain.

The higher magnifications of area A in Figure 3(b) and of area B in Figure 3(c) make the identification of the minerals possible. In the upper middle section in Figure 3(b) is a large partially dissolved grain whose edge is cracked. Actually it consists of two different compositions, one that appears slightly darker than the light gray of matrix and the other is black. The black is the quartz grains, and the lighter areas, represented here by spot 1145 and 1148 nearby left, show a composition typical of K-rich feldspar (Table 1). Such aggregates of quartz and feldspar (granophyric intergrowth) occur in almost all glazes of inlaid celadon from Kangjin. More dramatic images are presented in Figure 4(a-1) and Figure 4(a-2) of the shard 172 (S-14-1) whose glaze appears much more vitrified and clearer than that of the shard 166 (S-27-6) in Figure 3. The magnified image in Figure 4(a-2) shows such clusters of intergrowth around and even underneath the large bubble. Here it is shown clearly that the areas of feldpars melted, while the refractory quartzites remained almost intact during the firing.

The white grains in Figure 3(b) are determined to be wollastonite ($CaSiO_3$, 1144 in Table 1). In Chinese celadon these minerals, devitrified during the cooling process, are found rather abundantly, but it is rarely observed in Korean celadon glaze.[13] The lack of this mineral could be an indication that cooling took place more quickly in Kangjin kilns, usually smaller than Chinese ones.

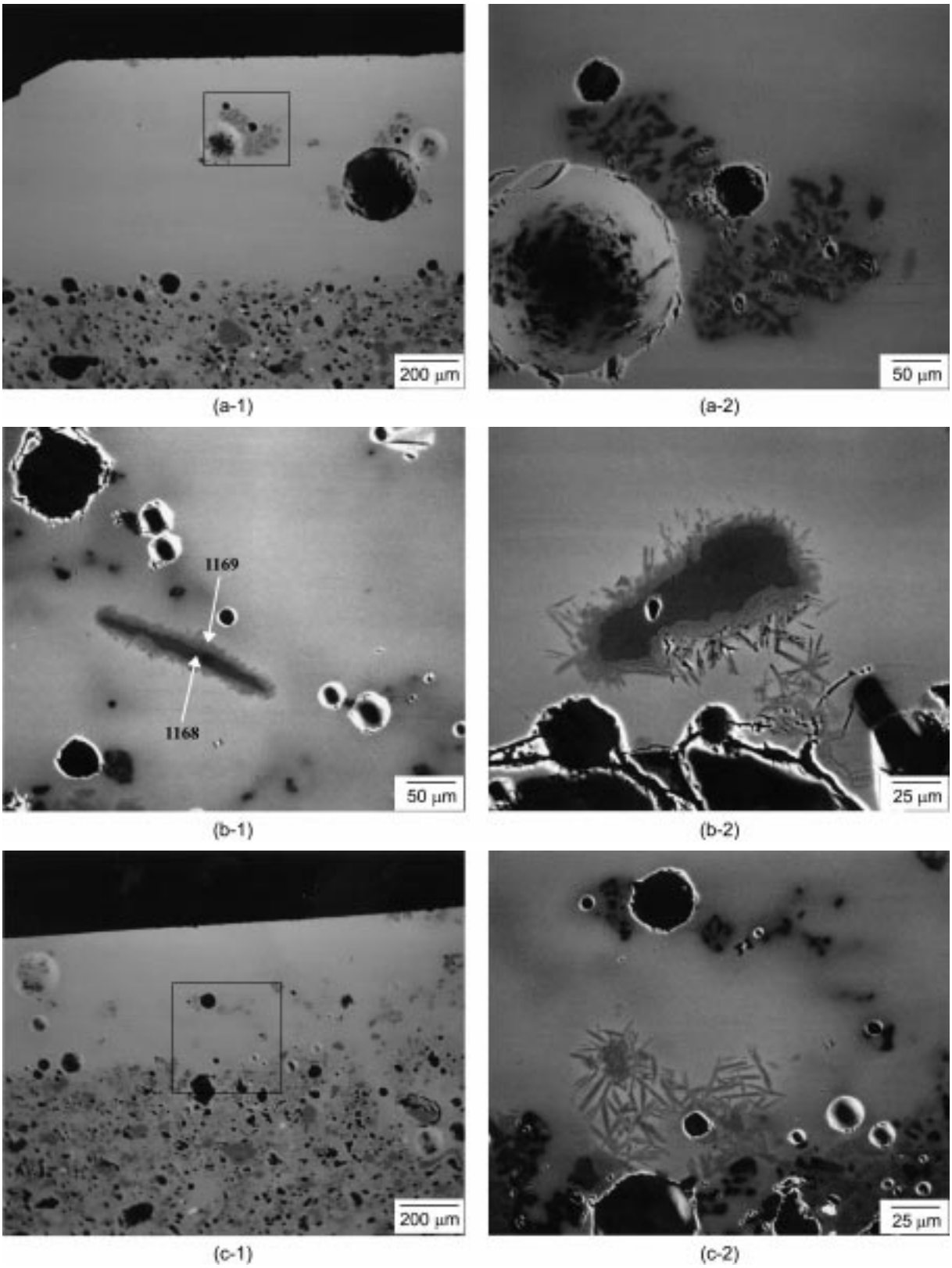

Figure 4. Backscattered electron images of fine quartz grains and other crystals in the glaze and the interface. (a-1) 172 (S-14-1); (a-2) A higher magnification of the boxed area in (a-1); (b-1) 169 (S-27-9); (b-2) 171(S-14-1); (c-1) 174(S-10-4); (c-2) A higher magnification of the boxed area in (c-1).

In Figure 3(b) is yet another remnant mineral pointed out here by the letter M next to the crackle on the right-hand side and also in Figure 3(c). This elongated mineral occurs often in Kangjin glaze, as shown additionally in Figure 4(b-1) and Figure 4(b-2). Usually the rim of this relict mineral is dissolved and with the matrix material a new mineral of needle shape is devitrified. Its EPMA measurement shows that the point 1168 in the core has the muscovite composition [$KAl_2(AlSi_3O_{10}(OH)_2)$] of high aluminum and potassium oxides, and the point 1169 on the rim of the needle-shaped mineral has composition close to that of anorthite ($CaAl_2Si_2O_8$).

Ca-rich feldspar anorthite is formed when high Ca area comes into contact with high aluminum area, as is the case above between the muscovite and glaze. Thus, often this mineral devitrifies along the glaze interface with body or white inlay. In Figures 3(b), 3(c), and 4(c-1) the presence of this mineral is only suggested along the glaze-body interface,

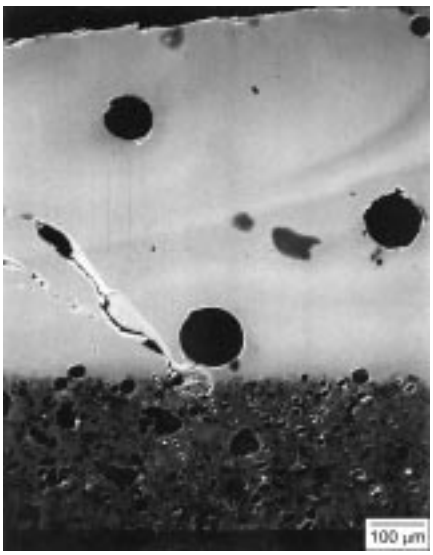

Figure 5. Backscattered electron image of schlieren effect, an occurrence of dark and light contrasting areas, caused by inhomogeneousness of glaze composition in shard 22 (CE11-3).

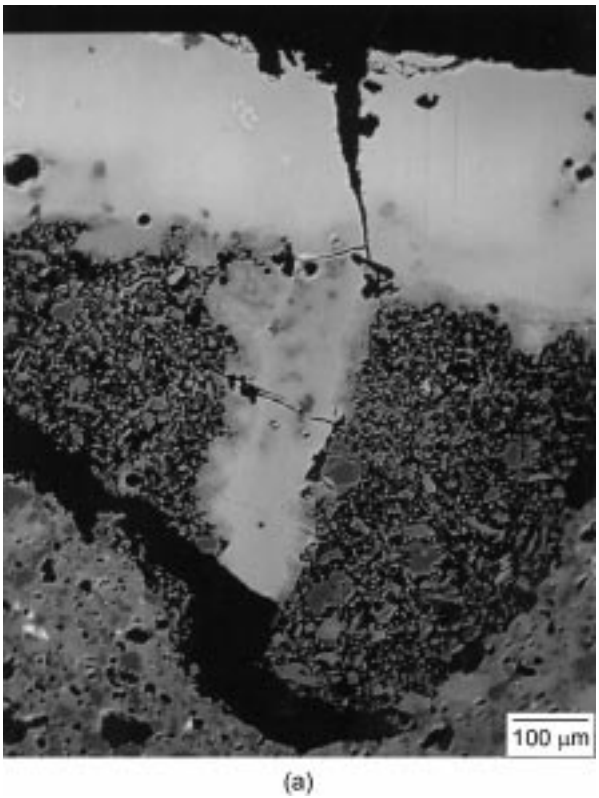

Figure 6. Backscattered electron images of white inlay in relation to glaze and body. (a) 19 (CI11-2); (b) 22 (CE11-3); (c) 166 (S-27-6).

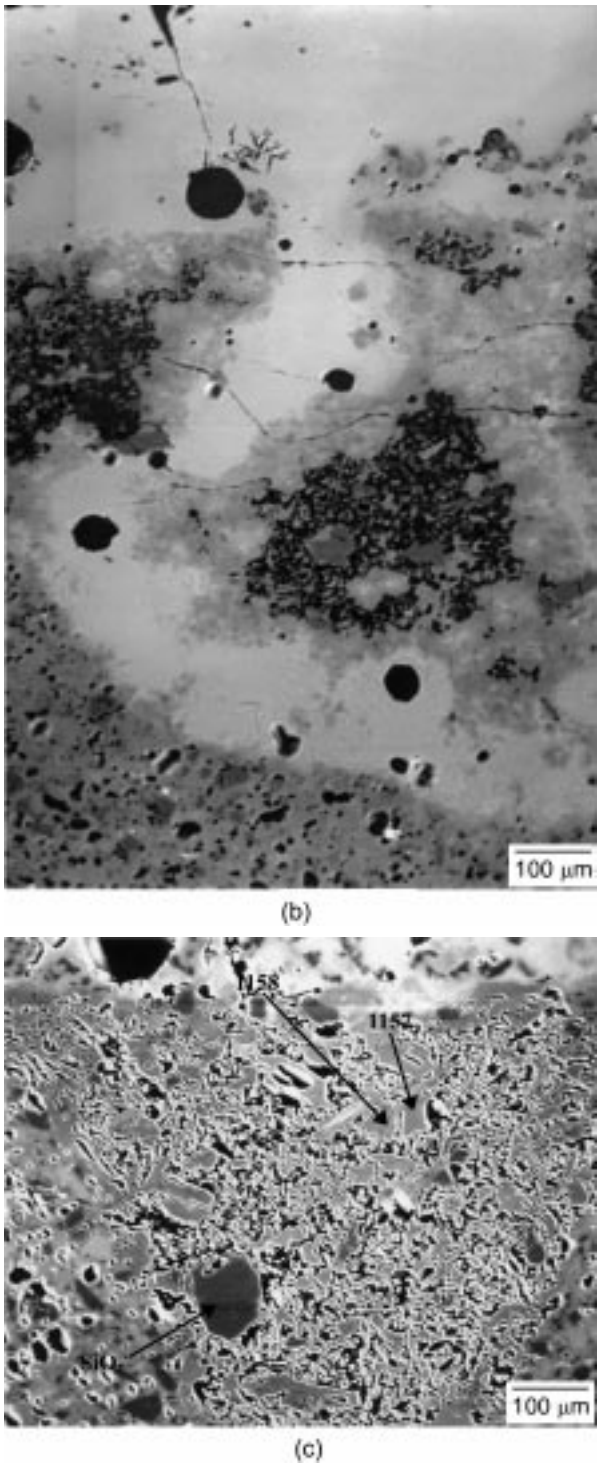

Figure 6. Continued.

but in the more magnified picture of Figure 4(c-2) the anorthite needles are clearly observed near the interface along with small bubbles and aggregates of quartzites.

Another characteristic that stands out in the celadon glaze is the schlieren effect, which results from inhomogeneous state of the glaze mixture. Slight differences in composition are manifested as dark (from areas with lighter elements) and light strips (from areas with heavier elements), creating wave image in BEI in Figure 5. If glaze were fired longer, small heterogeneities would have resulted in homogeneous glass matrix. A somewhat short firing schedule and inadequate mixing are likely to have been deliberately chosen to create such a ripple effect, which in combination with various mineral grains and bubbles interacts with light resulting in depth and rich texture.

White Inlay. Three pictures in Figure 6 show the overall

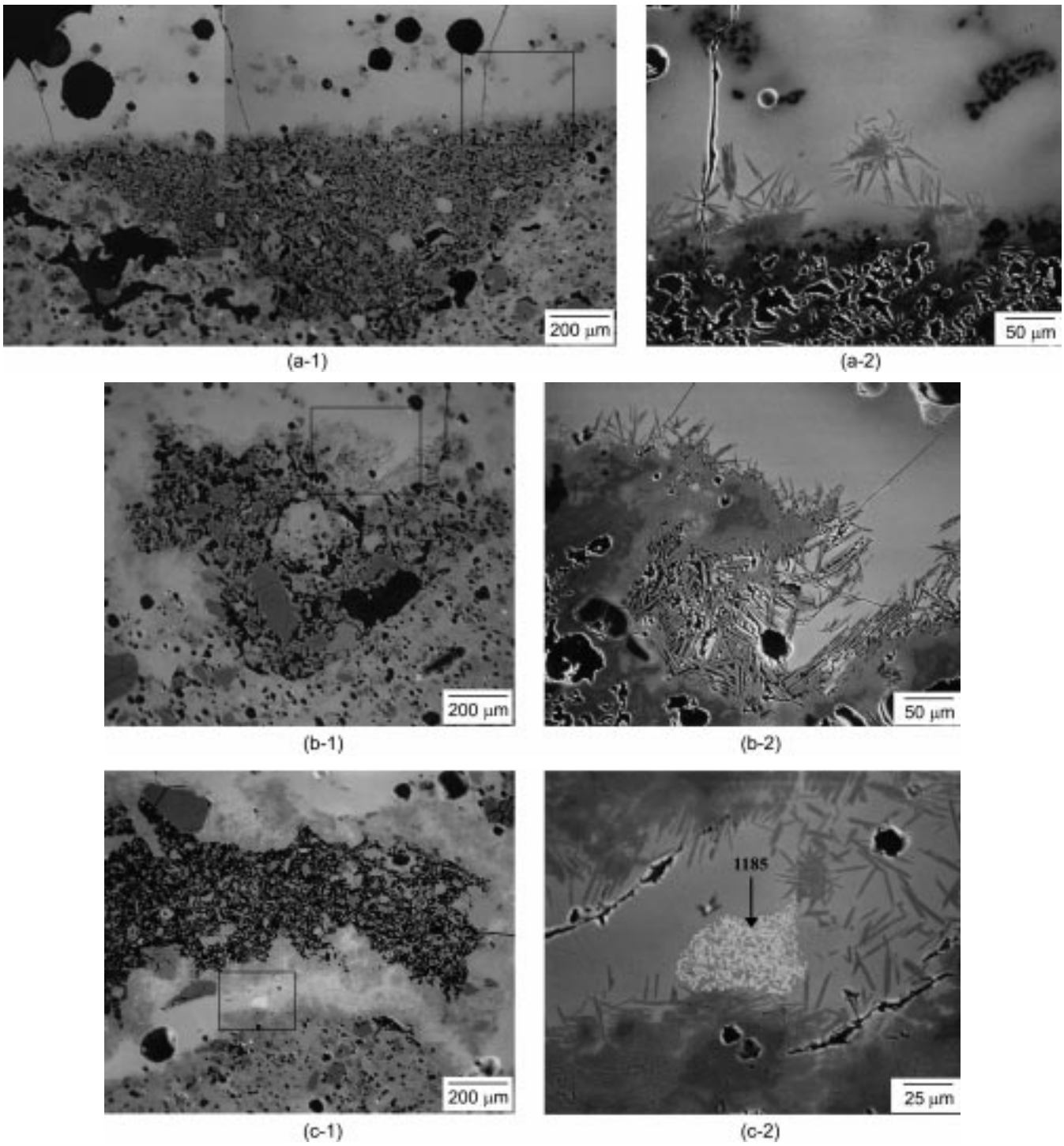

Figure 7. Backscattered electron images of fine crystals in white inlay and in the interface between glaze and white inlay. (a-1) 174 (S-10-4); (a-2) A higher magnification of the boxed area in (a-1); (b-1) 171 (S-14-1); (b-2) A higher magnification of the boxed area in (b-1); (c-1) 22 (CE11-3); (c-2) A higher magnification of the boxed area in (c-1).

structural relationship of the white inlay with the glaze and the body. Most of the inlay is triangular as seen in these pictures, but some are tabular line, running parallel to the glaze. The shards in Figures 6(a) and (b) are typically vitrified, while Figure 6(c) shard is substantially under-fired. The inlay is usually even less vitrified than body due to its high

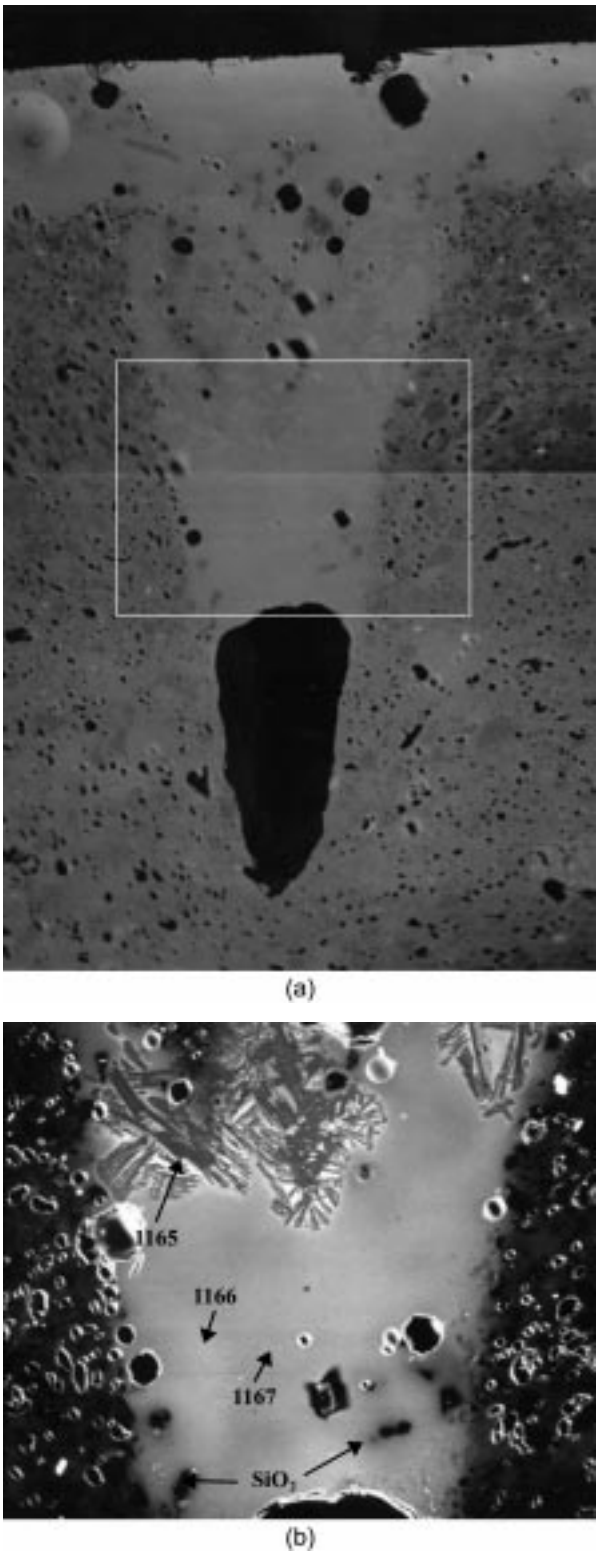

Figure 8. Backscattered electron images of black inlay. (a) 169 (S-27-9); (b) A higher magnification of the boxed area in (a).

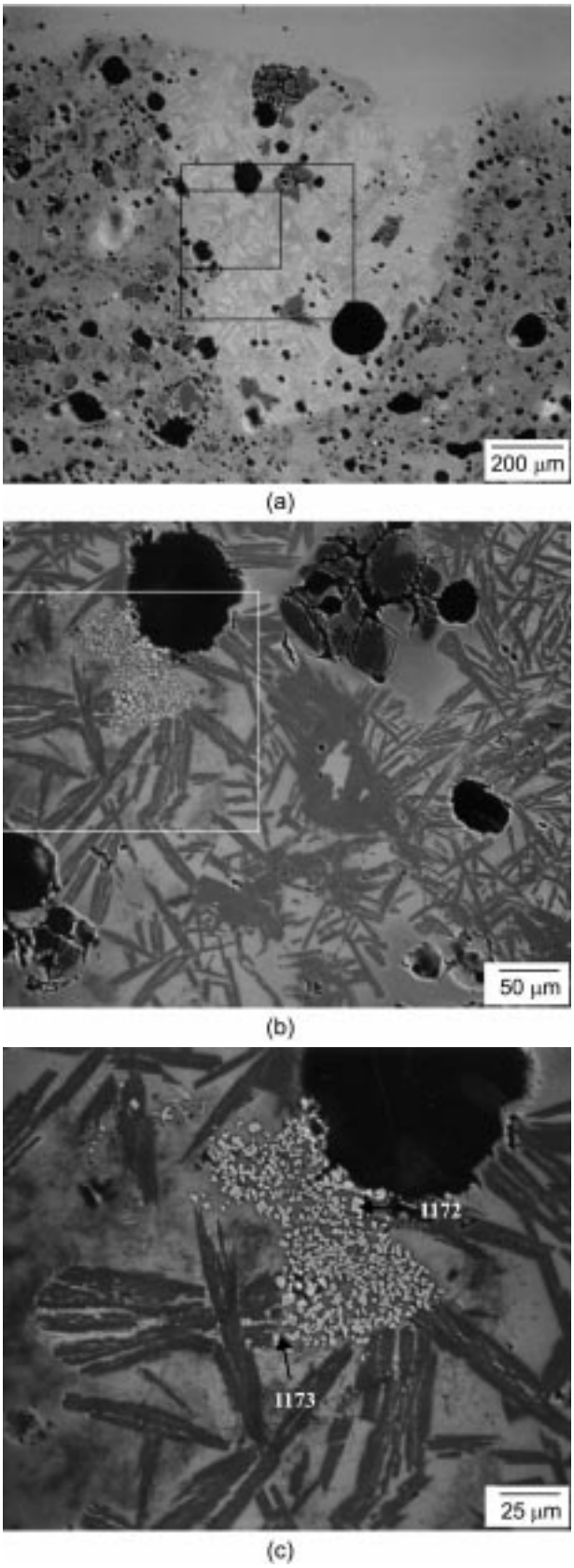

Figure 9. Backscattered electron images of fine crystals in black inlay of 22 (CE11-3). (a) Black inlay in relation to glaze and body; (b) A higher magnification of the area indicated by larger rectangle; (c) A higher magnification of the area indicated by the smaller rectangle.

content of aluminum oxide, between 30 to 40 wt.%, compared with about 20 wt.% in the body material. Muscovite mineral grains, such as 1157 and 1158, are preserved in near-original composition (Table 1) in the less vitrified sample in Figure 6(c) and are partially responsible for the higher clay content in inlay material.

Potters' speedy action of the filling often left some areas only sparsely filled or even empty like the dark left edge in Figure 6(a). The glaze seeped through some of these empty or sparsely filled spaces, creating "intergrade" sections of the white areas of similar appearance as the glaze in more vitrified samples. Only one such area is developed in the middle of inlay in Figure 6(a), but several places, including the backside, are developed in Figure 6(b). In Table 1 the comparison of EPMA measurements reveals the intermediate nature of intergrade composition between the glaze and regular areas of white inlay. As shown by the thread-like lines in Figures 6(a) and 6(b), these intergrades are usually cracked during the cooling process due to the mismatch in the expansion coefficients of the surrounding materials. Also the intergrade area often leads to cracks in the glaze, as is the case in Figure 6(a).

In the three sets of two pictures each in Figure 7, micro-crystals are shown both in the overall relation to glaze (a-1, b-1, c-1) and more focused in higher magnification (a-2, b-2, c-2). Needles of calcium feldspar anorthite are devitrified extensively in the interface between the Ca-rich glaze and Al-rich white inlay as was the case between the glaze and body. The needle shapes are gathered delicately like flowers in Figure 7(a-2), massively aggregated in Figure 7(b-2), and occur in individual rod forms in Figure 7(c-2). The cluster of white grains in Figures 7(c-1) and 7(c-2) (1185 in Table 1) in the backside intergrade is a mineral of apatite composition [$Ca(PO_4)O_3(OH, F, Cl)$]. This Ca and phosphate mineral is likely to occur in wood ash, a main component of celadon glaze, but it is rarely as well preserved in Koryŏ celadon, as shown here.

Black Inlay. In backscattered electron images of Figures 8 and 9 the black inlay appears very similar to the glaze. There is hardly any interface between the glaze and the inlay in Figure 8(a). This contrasts strikingly with white inlay, which was much less vitrified than either the glaze or body. The difference is naturally due to the compositions of two types of inlay. Compared with white inlay, typical matrix spots as 1166 and 1167 in Figure 8(b) of black inlay have a much lower content of aluminum oxide, around 20 wt.%, much higher content of iron oxide, around 12 wt.%, and higher content of calcium, above 5 wt.% (Table 1). Phosphorous and manganese oxides, found in the ash component of glaze, are also present in black inlay. Similarity between glaze and black inlay in composition and microstructure suggests that black inlay was formulated by adding a black clay component, such as biotite, to glaze material.

The incision for the black inlay in Figure 8(a) is so deep that its tip is understandably left empty and appears black in the backscattered electron image. Higher magnified image in Figure 8(b) shows the same microstructural features in the inlay as in the glaze. Aggregates of tiny quartz grains are found in areas ever so slightly darker than the average matrix. As in glaze the darker areas represent quartz-feldspar intergrowth, whose feldspar portion has melted but not yet vitrified and mixed completely into matrix.

As was expected from the appearance of needle shapes, 1165 spot is high in calcium and in aluminum, showing that it is anorthite crystal (Table 1). This mineral occurs as commonly in black inlay as in glaze. In fact, it is devitrified in such abundance in inlay shown in Figure 9 that even in smaller magnification in Figure 9(a) crystal needles are seen all over the inlay. The cluster of white grains in Figures 9(b) and 9(c) has spinel compositions of $MgO\text{-}Fe_2O_3$. Rather abundant occurrence of such spinel grains is an interesting characteristic feature of the black inlay used in the Kangjin celadons.

Conclusion

The body images of two irregularly mixed matrix phases are similar to those in the Chinese celadons from Jingdezhen.[14] The mixture of muscovite clay component and feldspars in *tosuk*, the *tanmi* material of the inlaid celadon, is reflected in such images.

Images of glaze include bubbles of various sizes, remnant muscovite minerals, quartz minerals cracked around the rims, composite minerals of quartzite grains in the mist of melted feldspar, and devitrified anorthite crystals. These and the schlieren effect from the inhomogeneous mixing of the glaze material are responsible for the deep translucent soft appearance of glaze.

The incised areas of white and black inlay are often left empty or only sparsely filled. In white inlay, glaze seeped through some of these areas forming intergrade of intermediate composition between the white inlay and the glaze. Needle-shaped anorthite crystals are formed in the interface between the inlay and the glaze and also in intergrade areas. The high content of aluminum, above 35 wt.%, and remnant muscovite minerals suggest *tosuk* as an important component for the inlay as it is for the body. Kaolinite type clay with only a small amount of iron impurity might have been added to the *tosuk* body material.

The close similarity in the microstructural features between the black inlay and glaze suggests that glaze was used together with biotite clay that contains much iron oxide as the inlay material. Extensive amounts of anorthite and the aggregates of spinel grains of $MgO\text{-}Fe_2O_3$ composition are found in the inlay.

As seen in this work backscattered electron images and the EPMA compositional measurement of distinct micro-areas lead to important information about the production technical parameters. This is one of several reports on many images and detailed descriptions that the authors are preparing from several hundreds of optical and electron microscopic images and micro-compositional measurements taken on Korean traditional ceramics. Such a systematic presentation is expected to reveal much about not only Korean ceramics, but also

their developmental relationship with Chinese and Japanese technology.

Acknowledgement. We would like to thank David Lange of Hoffman Geological Laboratory at Harvard University for making microstructural identification and EPMA compositional measurements. We would also like to acknowledge with gratitude the excavation team from Haegang Ceramics Museum, especially Mr. Kun Choi, for providing us the shards excavated in Kangjin.

References

1. Kingery, W. D. *Ceramics and Civilization*; Kingery, W. D., Ed.; American Ceramic Society: Westerville, Ohio, U.S.A., 1986; Vol. 3, p 153.
2. Hangst, K. *Celadon Wares of the Koryo Period, 918-1392*; Choi-Bae, S., Ed.; Museum für Ostiatische Kunst: Cologne, Germany, 1984; p 233.
3. Vandiver, P. B.; Cort, L. A.; Handwerker, C. *Ceramics and Civilization*; Notis, M. D., Ed.; American Ceramic Society: Westerville, Ohio, U. S. A., 1989; Vol. 4, p 347.
4. Newman, R. *Materials Issues in Art and Archaeology II* (*Mat. Res. Soc. Symp. Proc. Vol. 185)*; Vandiver, P. B.; Druzik, J., Ed.; Materials Research Society: Pittsburgh, Pennsylvania, U. S. A., 1991; p 429.
5. Koh Choo, C. K. *Materials Issues in Art and Archaeology III (Mat. Res. Soc. Symp. Proc. Vol. 267)*; Vandiver, P. B. *et al.*, Eds.; Materials Research Society: Pittsburgh, Pennsylvania, U. S. A., 1992; p 633.
6. Koh, K. *J. Korean Hist. of Sci. Soc.* **1992**, *14*, 23.
7. Koh Choo, C. K. *Archaeometry* **1995**, *37*, 53.
8. Koh Choo, C. K.; Kim, S.; Kang, H. T.; Do, J. Y.; Lee, Y. E.; Kim, G. H. *Archaeometry* **1999**, *41*, 51.
9. Lee, Y. E.; Koh, K. *J. Korean Chem. Soc.* **1998**, *42*, 251.
10. Koh Choo, C. K.; Kim, K. H.; Lee, Y. E.; Kim, J. S. *Archaeometry* **2002**, *44*, 199.
11. Lee, Y. E.; Koh, K. *J. Korean Chem. Soc.* **2002**, *46*, 125.
12. T'ae-p'ing Lao-jên (Song dynasty), *Hsui-chung-chin* in *Hsüeh-hai Lei-pien*, by Ts'ao Jung (1613-1685), printed in 1831 (in Chinese).
13. Vandiver, P. B. *The Radiance of Jade and the Clarity of Water-Korean Ceramics from the Ataka Collection-*; Itoh, I.; Mino, Y., Organized; The Art Institute of Chicago: Hudson Hills Press: New York, U. S. A., 1991; p 151.
14. Tite, M. S.; Freestone, I. C.; Bimson, M. *Archaeometry* **1984**, *26*, 139.